Photophysics of *Ds*Red, a Red Fluorescent Protein, from the Ensemble to the Single-Molecule Level

B. Lounis,‡ J. Deich, F. I. Rosell, Steven G. Boxer, and W. E. Moerner*

Department of Chemistry, Stanford University, Stanford, California 94305-5080

Received: December 31, 2000; In Final Form: March 23, 2001

*Ds*Red, a tetrameric fluorescent protein cloned from the *Discosoma* genus of coral, has shown promise as a longer-wavelength substitute for green fluorescent protein (GFP) mutants for in vivo protein labeling. Bulk and single-molecule studies of the recombinant protein revealed that the *Ds*Red chromophore shows high stability against photobleaching as compared to GFP mutants. Stark modulation spectra confirm that the electronic structure of the *Ds*Red chromophore is similar to that of GFP. However, the tetrameric nature of *Ds*Red leads to intersubunit energy transfer, as evidenced by the molecule's unusually low fluorescence anisotropy when immobilized (0.23 ± 0.02). This value is approximately consistent with an estimate of the energy transfer rates based on preliminary crystallographic information. The fluorescence emission bleaches at a rate linear in the applied excitation intensity, implying that the cessation of emission during pumping at 532 nm is light-driven and, consistent with the tetrameric structure, several photobleaching "steps" were observed for individual complexes. Because more photons are emitted before bleaching, this study suggests that *Ds*Red may be superior to some GFP-based labeling technologies as long as tetramerization is not an issue in physiological studies.

Introduction

Single-molecule spectroscopy (SMS) continues to play a unique role in the elucidation of the dynamics of an increasingly broad range of complex systems.[14,25] By removing the averaging inherent in ensemble measurements, SMS yields a measure of the distribution of molecular properties which is of importance in systems that display static or time-dependent heterogeneity. Concurrently, developments in fluorescence microscopy have made the observation of single molecules of biological interest possible under a wide range of experimental conditions.[26] This versatility can be exploited to examine the molecular complexity of many biological systems.

One critical challenge to the application of SMS techniques to biomolecules, especially in vivo, is the introduction of a fluorophore that acts as a reporter of activity, local environment, or spatial location. While certain important proteins display useful amounts of visible fluorescence arising from native cofactors,[12] most require the attachment of an extrinsic fluorophore to serve as the probe. The genetic fusion of naturally fluorescent proteins to a protein of interest ensures a consistent 1:1 stoichiometry in the cell, without the need for external chemical reactions. While the green fluorescent protein (GFP) and its mutants have proved suitable for many applications,[22,27] the relatively high quantum yield of photobleaching ($\sim 10\times$ that for a rhodamine dye[16]) leaves room for improvement in applications that require a large number of emitted photons, such as in single-molecule studies. Also, no mutant of GFP has been demonstrated to be a strong emitter at long (>550 nm) wavelengths, where the interference from endogenous fluorophores is substantially less severe.

Considering these issues, the discovery of a highly fluorescent red protein from the *Discosoma* genus of coral,[13] *Ds*Red (originally termed drFP583), has aroused intense interest.[7] The protein is a superior emitter at long wavelengths when compared with GFP and its mutants, with a monomer molar extinction coefficient of 75 000 L mol^{-1} cm^{-1} at 558 nm and a 70% fluorescence quantum yield.[1] Recent fluorescence correlation spectroscopy (FCS)[8] and analytical ultracentrifugation studies[1] have provided strong evidence that the protein is tetrameric even at nanomolar concentrations. With wild-type emission at 583 nm, and the possibility to shift the fluorescence to longer wavelengths (and even to inhibit tetramerization) through strategic mutagenesis, *Ds*Red may become the cellular reporter protein of choice. This paper explores the dynamics of this fluorophore at both the ensemble and single-molecule level to assess the utility of this protein over a range of experimental conditions.

Materials and Methods

Construction of pRSET$_b$-RED. The 777-bp, *Bam*HI−*Stu*I fragment from the plasmid p*Ds*RED (Clontech) was ligated to the 2.9-kbp *Bam*HI−*Pst*I fragment of pRSET$_b$-wtGFP. The resulting 3.68-kbp plasmid (pRSET$_b$-RED) thus encodes *Ds*Red with a *N*-terminal poly-histidine purification label under control of the T7 promoter. The amino acid sequence between the initiator Met and the first residue of *Ds*Red is M−R−G−S−H−H−H−H−H−H−G−M−A−S−M−T−G−G−Q−Q−M−G−R−D−L−Y−D−D−D−D−K−D−P−R−V−P−V−A−T-*Ds*Red.

Protein Preparation. Poly-His tagged *Ds*Red was expressed in *Escherichia coli* BL21DE3pLys::pRSET$_b$-RED with a 5-L BioFlo 3000 fermentor (4.3 L $2\times$ YT,[19] 100 mg ampicillin/L, 0.01% antifoam agent (BASF DF204), 12 h at 37 °C plus 8 h at 30 °C after addition of IPTG to ~0.5 mM). The cells were

‡ Permanent address: CPMOH, Université Bordeaux I, 33405 Talence, France.

* To whom correspondence should be addressed: Phone: 650-723-1727; fax: 650-725-0259; e-mail: moerner@stanford.edu.

10.1021/jp010116x CCC: $20.00
Published on Web 05/09/2001

lysed with a French press, and the protein was batch extracted from the cleared supernatant fluid by metal affinity chromatography with Ni-NTA agarose (Qiagen) equilibrated in cell breaking buffer (50 mM HEPES buffer, pH 7.9, 300 mM sodium chloride). The immobilized protein was washed and then eluted from the column with 20 and 200 mM imidazole, respectively, then concentrated and dialyzed overnight in 50 mM HEPES buffer, pH 7.9, before further concentration and storage at −71 °C.

Native *Ds*Red was expressed constitutively in *E. coli* DH5α:: p*Ds*RED (1 L LB broth [19] in 6 L conical flasks, 100 mg/L ampicillin, 37 °C, 24 h). After harvest, these cells were treated with PMSF, lysozyme, DNaseI, and RNaseI (0.1 mM, 100, 5, and 1 mg/100 g of cell pellet, respectively, 1 h, 4 °C), and lysed with two cycles of freezing in liquid nitrogen and thawing on ice. The protein was batch extracted from the cleared supernatant fluid with Q-Sepharose equilibrated in 10 mM HEPES buffer, pH 7.9. The protein was purified further with a fresh ion exchange chromatography column from which it was eluted with a linear sodium chloride gradient (0−100 mM salt/300 mL). The central fractions of the single colored peak were pooled, concentrated, and subjected to size exclusion chromatography with Sephadex G100-superfine (2 × 100 or 1 × 80 cm) equilibrated in dilute buffer. Fractions with an absorbance ratio $A_{558}/A_{280} > 1$ were collected and concentrated for storage at −71 °C. The purity of these samples was assessed by SDS−PAGE (10% gel). Both the native and poly-His versions were utilized for measurements, with no significant difference observed between them. All protein concentrations were determined from the absorbance of each sample at 558 nm using the extinction coefficient from ref 1.

Ensemble Spectroscopy. Absorbance spectra were recorded either on a Lambda 12 or a Lambda 19 UV/Vis/NIR spectrophotometer (Perkin-Elmer); fluorescence spectra and anisotropies were obtained with a Fluoromax 2 (Instruments S. A.), with an excitation and emission bandwidth of 2.0 nm. Circular dichroism spectra (∼10 μM protein in ∼5 mM HEPES buffer, pH 7.9) were measured at 25 °C between 400 and 650 nm with an AVIV spectropolarimeter model 62A DS equipped with 0.1- or 1.0-cm path length quartz cuvettes. The Stark spectrum of *Ds*Red with and without a poly-His purification tag was measured at 77 K essentially as described elsewhere.[3] Fluorescence lifetimes were obtained with a standard time-correlated-single-photon counting device (Picoquant Time Harp), using a frequency-doubled femtosecond Ti-sapphire laser (Coherent) to provide illumination at a wavelength of 445 nm. To examine chromophore photobleaching, the emission from a 2.0% agarose gel containing 1 μM *Ds*Red was monitored as a function of time. Various powers of circularly polarized 532 nm illumination were focused on the sample in epifluorescence mode, and the total emission intensity was recorded as a function of time (typical integration time of 100 ms). Separately, the fluorescence spectra of *Ds*Red (2 mL of a 300 nM solution in a sealed cuvette) were examined before and after photobleaching for 9.25 h with a 4.4 W beam of 532 nm light from a doubled Nd:YAG laser (Spectra Physics) which was expanded to illuminate the entire cuvette. This experiment was designed to complete essentially the "fast" portion of the photobleaching (see Results) and to determine if different absorbing products built up during prolonged irradiation.

Single-Molecule Spectroscopy. All SMS measurements were performed in buffer A (5 mM each MES, potassium phosphate, HEPES, sodium borate, and CAPS buffers, pH 6.0, 75 mM sodium chloride) unless otherwise specified. For microscopy samples that require confinement of the *Ds*Red, agarose gels (100−200 nm estimated pore size[17]) were employed to provide a largely aqueous matrix. 2.0% agarose (w/v, from Boehringer Mannheim) was melted, cooled slowly to 37 °C in a water bath, mixed thoroughly with protein solution, and incubated for 15 min at 37 °C. This solution was diluted in 2% agarose to a final protein concentration of 1 nM, and 5 μL of it was sandwiched between two 22 × 22 mm glass coverslips and allowed to cool to produce a ∼10 μm thick sample. All coverslips used in this work were cleaned extensively before use with sequential treatment with detergent [1% RBS (Pierce) in warm 50% ethanol], water, acid [1% (w/v) Nochromix (Aldrich) in concentrated H_2SO_4], water, and spectroscopic grade methanol, and dried with a nitrogen stream.

Samples were mounted on a Nikon TE300 inverted microscope and illuminated with 532 nm light from a frequency doubled Nd:YAG laser (Spectra Physics) through a rear epifluorescence port by reflection from a 540DRLP dichroic mirror (Omega Optical). A 60 × 1.4 NA PlanApo oil-immersion objective focused the light onto the sample. For epifluorescence observations, a region 10 μm in diameter was illuminated, and data were collected in the center of this region to minimize the effects of spatial variation in the intensity. When the illumination was switched from epifluorescence to confocal mode, the emission was focused through a 50 μm pinhole, and a Nano-Drive piezoelectric scanning stage (Mad City Labs) was used to scan 20 × 20 μm regions of the sample with 100 × 100 pixels resolution. The emission was filtered through a 580DF30 band-pass filter (Omega Optical) before detection with a Si avalanche photodiode (EG&G, SPCM, 25 cps dark counts) used as a photon counter.

Results

Protein Characterization. The room-temperature absorption spectrum of native *Ds*Red is very similar to previous reports.[13] In contrast to these reported data, however, the ratio A_{558}/A_{280} was 1.2 instead of ∼2, suggesting that the protein was not completely pure. From SDS−PAGE analysis after a second cation exchange chromatography step, it was estimated that the purity of the samples was better than 90%, but the absorbance ratio remained unchanged. Also, three bands were always encountered in denaturing electrophoresis gels which correspond to protein monomers and to hydrolysis fragments consistent with Gross et al.[7] The addition of the *N*-terminal poly-His tag to *Ds*Red did not affect the absorption spectrum of the protein appreciably, but by accelerating the purification, it became possible to examine the protein sooner after cell lysis. In these early stages, the absorption shoulder at 482 nm appears as a better resolved feature along with a weaker band at 408 nm. Both features are associated with an immature chromophore.[7] With time (∼8−12 h after cell lysis), these features diminished or disappeared altogether as the chromophore reached maturity. The features associated with immature chromophores were absent in the samples used for the single-molecule experiments. One cannot rule out the possibility that the low A_{558}/A_{280} ratio might be due to tetramers in which the chromophores in, for example, 3 of the 4 subunits are mature while in the remaining subunit the chromophore has not developed at all. Such hypothetical tetramers would have a visible absorption characteristic of pure mature chromophores but an A_{558}/A_{280} ratio that is low (see also the anisotropy discussion below).

Ensemble Photophysical Properties. In the visible region of the CD spectrum (data not shown), *Ds*Red exhibits positive ellipticity centered at 515 and 485 nm, and a negative Cotton

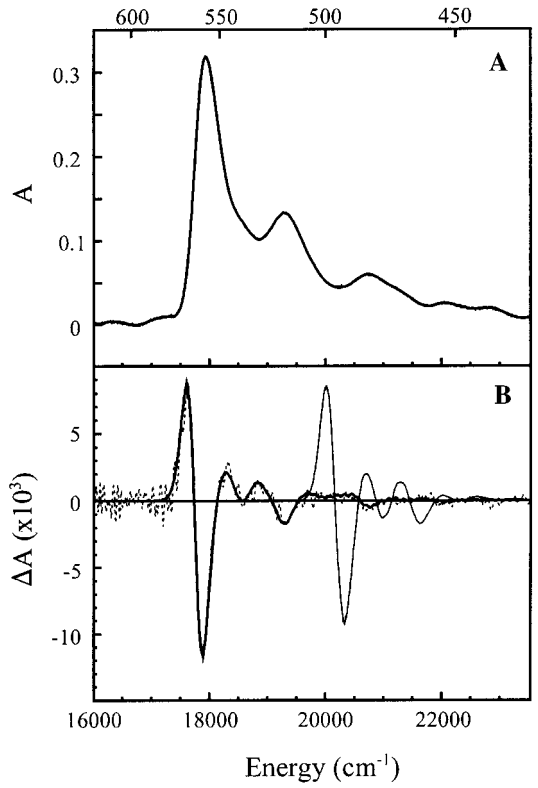

Figure 1. (A) Absorption spectra of DsRed at 77 K (20 mM HEPES buffer, pH 7.9, 50% glycerol). (B) Comparison of the Stark spectra of DsRed (bold, solid curve) and the S65T variant of GFP (light, solid curve) measured at 77 K (conditions as in panel A above) normalized to 1 MV/cm. The second derivative of the absorption spectrum measured at 77 K is illustrated with dotted curve.

effect at 570 nm. These features are broad and lack the symmetric split (positive and negative ellipticity) that is observed when two oscillators are coupled in resonance by virtue of the electrostatic interaction between their corresponding transition dipoles.[4] On the basis of the recently reported X-ray structure of the tetramer,[18] the interchromophore distances are too large for a chiral exciton interaction.

At 77 K, the three principal bands in the absorption spectrum sharpen and shift to 559.6, 520.5, and 484.4 nm (Figure 1A). The Stark spectrum of *Ds*Red is compared to that of the S65T variant of GFP in Figure 1B; the band shape of the Stark spectrum of *Ds*Red is nearly identical to the second derivative of the absorption, as is observed for the B-state of wild-type GFP and the GFP mutant S65T.[2] Quantitative analysis of these data yield a change in the dipole moment $|\Delta\mu|$ between the ground and excited state of 7.0 D, and an angle ζ between the transition dipole moment and $\Delta\mu$ of 13°. Aside from the spectral shift between *Ds*Red and the S65T variant of GFP and some amplitude differences, the low temperature absorption and Stark spectra of the two proteins are virtually superimposable.

At room temperature, the excitation and emission spectra for *Ds*Red in buffer compare quantitatively with previous reports.[1,8] In searching for optimal experimental conditions for single-molecule detection of *Ds*Red, it was noted that the protein's photophysical properties are remarkably insensitive to its environment. In agreement with Baird et al.,[1] the fluorescence spectra are relatively unaffected by changes in pH from pH 5.0 to 10.3. However, samples prepared at pH 4.5 show a gradual loss of all fluorescence, with a rate that increases as the pH decreases further (data not shown). This loss was reversible over short time scales; raising the pH to 8 after 15 min by the addition

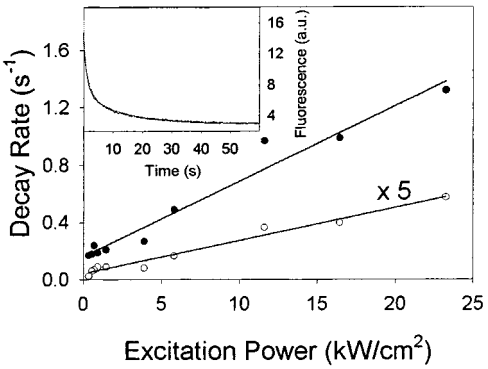

Figure 2. Photobleaching rates as a function of the applied light intensity (●, fast decay component; ○, slow decay component). The inset shows the fluorescence emission of a typical bulk sample during photobleaching at 3 kW/cm^2, demonstrating the biphasic nature of the decay. Fits to such decays with a sum of two exponentials yielded the decay constants in the central portion of the figure.

of buffer restored the original fluorescence. The fluorescence spectra are independent of buffering agent and ionic strength over a range from 50 to 1000 mM.

The quantum yield of fluorescence was determined by comparison with a standard of equal optical density, sulforhodamine 110 (Aldrich) in 95% ethanol, using the value of 0.93 reported by Soper et al.,[20] and correcting for the difference in refractive index between water and ethanol. The value obtained here (0.69 ± 0.03 when excited at 540 nm) is in excellent agreement with previous work.[1] Using pulsed excitation, measurements performed in both confocal and epifluorescence geometries yielded a fluorescence lifetime of 3.6 ± 0.1 ns for *Ds*Red in buffer A, in agreement with Heikal et al.[8]

Ensemble Photobleaching Experiments. Integration of emission spectra after >9 h bleaching revealed that the sample retained 28% of its original fluorescence between 550 and 650 nm. This residual fluorescence was unchanged after incubation in the dark, and the original emission could not be recovered by further intense illumination at shorter wavelengths, as reported for mutants of GFP.[6] Prolonged bleaching also generated a minor fraction of a new spectroscopic species with maximum absorption at 478 nm and weak emission at 499 nm.

Further examination of the bleaching behavior was accomplished with time-dependent epifluorescence microscopy of dilute protein samples ($\sim$1 μM) in agarose as a function of excitation power. All emission decays require at least a biexponential fit (inset, Figure 2). The two decay rates scale linearly with the applied power (Figure 2), demonstrating that the molecules were not near excited-state saturation and that no higher-order effects were relevant to these decay processes. Using the known extinction coefficients and the pumping rate, two photobleaching quantum yields were calculated: a faster bleaching probability (per photon absorbed) of 1.4×10^{-6} and a slower one of 1.2×10^{-7}. These values are comparable to those in ref 1, smaller than those in ref 8, and significantly smaller than the value measured for EGFP, $(8 \pm 2) \times 10^{-6}$.[16]

Ensemble Anisotropy Measurements. Because of the size of *Ds*Red tetramers (approximately 112 kDa), the rotational correlation time of the complex should be in excess of about 40 ns at room temperature as measured by FCS.[8] With such slow rotation as compared to the fluorescence lifetime, the fluorescence should not be depolarized unless internal energy transfer among nonparallel oscillators occurs. Measurements of the steady-state anisotropy reflect this, showing negligible decrease upon further increases in viscosity by the addition of

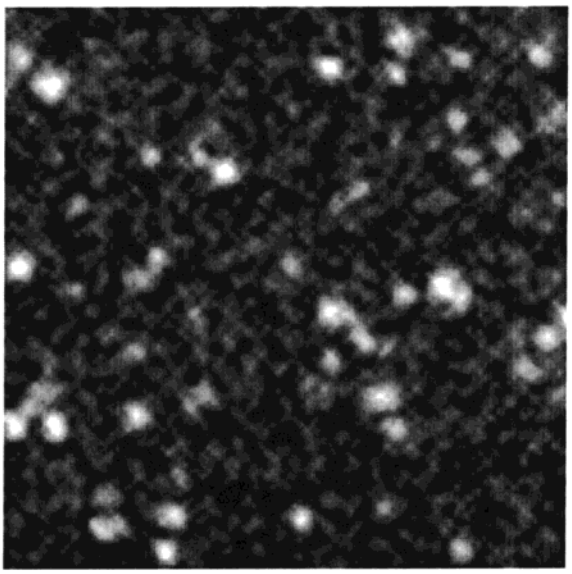

Figure 3. Confocal scanning microscopy image of the emission from isolated molecules of DsRed in agarose gel. The field covers a 20 × 20 μm range, 10 ms integration time per pixel, 100 × 100 pixels, with 4.5 kW/cm^2 pumping intensity at 532 nm.

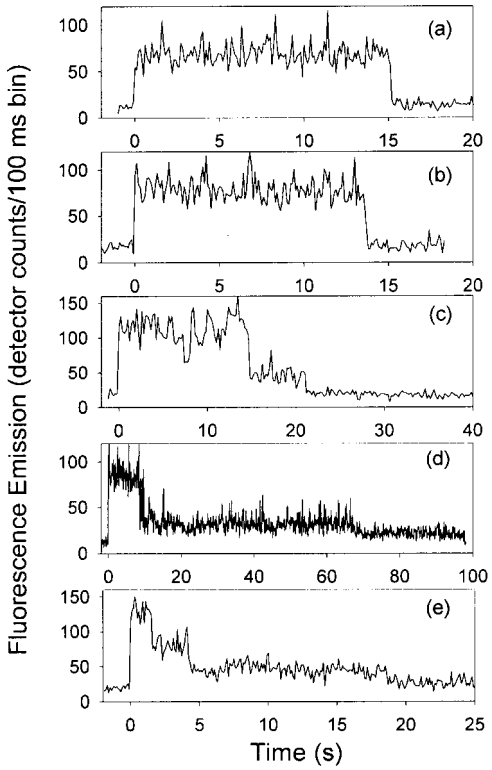

Figure 4. Typical examples of the fluorescence emission from single molecules of DsRed (detector counts per 100 ms) as a function of time. Included are molecules that bleached in one step (a,b), two unequal steps (c,d), and more than two steps (e). The excitation intensity was 9 kW/cm^2.

up to 50% glycerol to the buffer (data not shown). The measured anisotropy of the complex in buffer A is 0.23 ± 0.02 (three measurements by two different experimenters). The low anisotropy probably stems from energy transfer between the subunits of a tetramer (vide infra). This value is lower than that of GFP (0.37)[21] and also smaller than that reported for *Ds*Red at pH 9 (0.30)[8] for unknown reasons.

Single-Molecule Time Traces. Single-molecule fluorescence measurements were used to interrogate the emissive properties

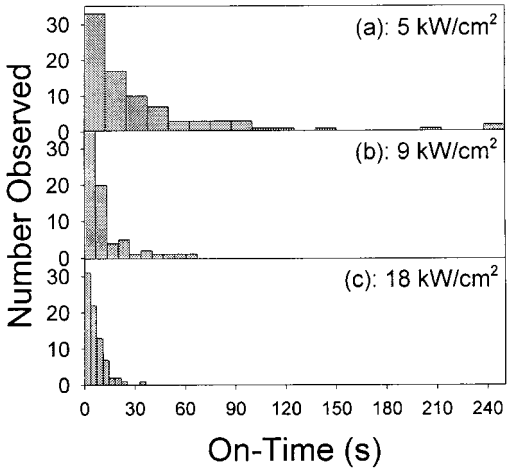

Figure 5. Histograms of the total time of emission for DsRed complexes at (a) 5 kW/cm^2, (b) 9 kW/cm^2, and (c) 18 kW/cm^2. Molecules that are exposed to higher excitation rates photobleach more quickly, demonstrating that the loss of fluorescence is due to a light-driven process and not to processes such as diffusion or conformational fluctuations.

of the chromophore in the absence of ensemble averaging. Emission from single molecules was located with standard confocal scanning microscopy as illustrated in Figure 3. The various isolated spots likely result from individual tetramers: for the concentration chosen (~1 nM *Ds*Red based on monomer) roughly 10−20 isolated protein complexes are expected in a given 20 × 20 μm area. Emission time traces were collected with the laser beam focused on each of 215 isolated single-molecule spots. Typical examples are shown in Figure 4. Taken together, the low concentration, the spot size used (~400 nm in diameter, near the diffraction limit), and the abrupt bleaching events (discussed in more detail below) demonstrate that the emission corresponds to individual protein complexes. At the intensities used (9 kW/cm^2), the background signal was due only to the dark noise of the detector and was the same as in samples without protein. Considering the complete set of single-molecule time traces, the intensity dropped either once (~45% of all cases, as in Figure 4a,b) or twice (also ~45%, as in Figure c,d), although three or four drops were recorded in ~10% of the traces analyzed (e.g., Figure 4e). Traces that displayed more than one drop (as in Figure 4c,d) typically exhibited a large first drop followed by a period of weaker fluorescence before complete photobleaching to the background level. The observation of several bleaching levels is conceptually consistent with the multimeric character of *Ds*Red. It is also possible that a fraction of the complexes have dissociated, but given that (a) K_d for the complex has been estimated to be less than 1 nM,[8] and (b) the members of a complex are trapped together in a small pore, it is likely that the tetrameric structure persists.

Further dynamical information may be extracted from the single-complex time traces. The "total on-times", i.e., the length of time during which a given complex emits light at any intensity level, were determined at several different excitation intensities and are displayed as histograms in Figure 5; the shape of these histograms is approximately exponential in character, as expected for an underlying Poisson process. The characteristic emission on-times decrease linearly as higher light intensities are focused upon the sample, demonstrating the photoinduced character of the process terminating the emission (i.e., bleaching). The linear increase in disappearance rate also suggests the absence of higher-order bleaching processes. At intensities of several kW/cm^2, *Ds*Red was observed readily for several

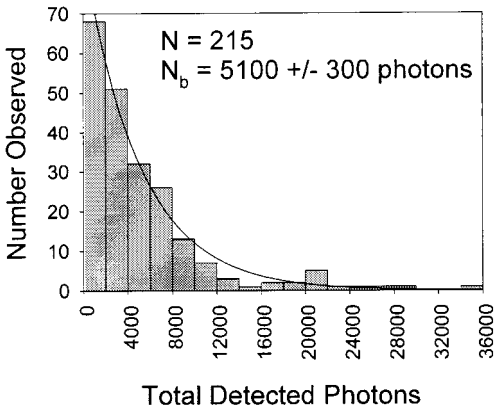

Figure 6. Histogram of the total number of photons detected from 215 individual DsRed complexes before photobleaching. The solid line denotes a single-exponential fit, where N_b is the characteristic photon number of the exponential.

seconds before photobleaching, in contrast to the few hundred milliseconds of observation reported for single EGFP at similar intensities.[16]

The total number of photons emitted for each single complex is another key parameter of a cellular or single-molecule reporter. Figure 6 shows a histogram of the results from 215 single molecules pumped with 532 nm light. The *Ds*Red molecules emitted comparable numbers of total photons (an average of 5100 detected photons) regardless of the intensity applied. This result also implies that the loss of emission is driven by the radiation applied, and caused by a process with a probability of occurrence which is linear with the number of emission events. This observation eliminates some bleaching mechanisms, such as those involving absorption from an excited state, and demonstrates that the molecules are not near excited-state saturation at the intensities studied. The histogram of total photon counts is consistent with a single population of emitters, as evidenced by the lack of secondary peaks in the frequency distribution.

Discussion

While this work was in progress, strong evidence that *Ds*Red exists primarily as a tetramer was obtained by biochemical methods,[1] the rotational correlation time,[8] and X-ray crystallography.[18] In this work, both the ensemble and single-molecule bleaching experiments suggest that the fluorescence of *Ds*Red is lost in stages. The ensemble studies show biexponential decay, and the single-molecule traces show between one and four sudden drops in intensity before returning to the original background fluorescence. Because the rate of bleaching varies linearly with the excitation power, such sudden, irreversible changes must be attributed to photochemistry, and not to any environmental effect. This linearity is also experimental proof that our pumping rate is well below that required for saturation of the target fluorophores, and thus we do not consider photophysical models which require simultaneous excitation of two fluorophores in one complex. Unexpectedly, however, most molecules (~90%) showed only one or two bleaching events, and multiple bleachings in the same complex were not of equal magnitude in terms of the change of fluorescence intensity. These results suggest that the monomers of the complex are coupled in some fashion, rather than independent emitters.

We consider three models that might explain the single-molecule results. First, at the extremely low concentrations used for the single molecule experiments (~1 nM), monomers, dimers, and tetramers may be trapped in the pores of the gel. Second, assuming tetramers, photochemical transformation of one or more of the four chromophores within the complex to a species whose absorption spectrum is shifted would lead to fewer molecules excited and consequently less emission. Third, still assuming tetramers, photochemical transformation of one or more of the four chromophores into a species that serves as a fluorescence quencher or trap for the emission of the unaffected chromophores could lead to decreased emission. These three possibilities (although more may be involved) are not mutually exclusive and cannot be rejected unambiguously based on the data available at this time.

Heikal et al. reported recently that the dissociation constant for a *Ds*Red tetramer is less than 1 nM.[8] Since our experiments are performed near this concentration, the precise value of K_d is important as it relates to the possible presence of dissociated species. Furthermore, because the single-molecule measurements are performed on species that are isolated in the pores of a gel, the bulk concentration is not defined. The relevant properties for the correct interpretation of our results in this case are the dissociation/association rates relative to rate at which the sample is diluted and trapped in pores. The entrapment of some fraction of the protein as monomers would provide a simple explanation for those traces that were observed to bleach in a single step. The presence of monomers could be tested by measuring the fluorescence anisotropy of such species. In this model, the number of "steps" for a given molecule's bright period might denote the number of monomers in that complex.

The second model describes the effect on the emission intensity of an isolated tetramer if there is a change in the absorption spectrum of one or more of the four chromophores. Because of rapid excited-state energy transfer relative to the excited state lifetime (see below), the emission is essentially equally likely to come from any of the four monomeric units. If the absorption spectrum of one of the chromophores changes due to some photochemical transformation, then the number of excited states that are resonant with the altered chromophore is reduced at the fixed excitation wavelength (532 nm). Assuming for simplicity that all chromophore pairs couple equally well, if the shift leads to a large reduction in extinction coefficient, then the shifted chromophore is not excited and the emission intensity would be reduced by one-quarter; if two chromophores are similarly damaged, the emission is reduced by half and so on. Because the change in extinction coefficient at the absorption wavelength need not be 100%, intermediate reductions in intensity can also be rationalized.

A third and possibly related model is that the emissive behavior results from the coupling of the four chromophores, with those that are damaged now acting as nonradiative quenching sites for neighboring monomers in the complex. In this model, the first period of high brightness corresponds to the fluorescence of an intact oligomer. After a period of excitation, at least one of the constituent fluorophores bleaches, and the residual fluorescence from the remaining intact chromophores is either negligible or greatly reduced by trapping on the damaged chromophore(s). The calculated rate of energy transfer between intact fluorophores within a complex is significantly faster than the rate of emission (see below). Therefore, if the damaged fluorophore still absorbs efficiently but emits poorly, it can act as a trap for the energy of the absorbed photon and provide a suitable pathway for dissipating the energy via means invisible to our detection methods. Similar multiple steps due to quenching effects in an electronically coupled system have been observed in single-polymer spec-

TABLE 1: Calculated and Measured Parameters for the Energy Transfer Model as Described in the Text

	1 ↔ 2	1 ↔ 3	1 ↔ 4	2 ↔ 3	2 ↔ 4	3 ↔ 4
k_{ij}/k_F	10.5	61.1	0.35	0.34	48.3	10.7
r_{ij}	−0.04	0.25	0.05	0.06	0.32	−0.04
κ_{ij}^2	0.56	1.73	0.01	0.01	1.54	0.58
d_{ij} (Å)	33.6	27.3	42.9	42.9	27.4	33.6

troscopy[23] and photosynthetic antenna complexes.[10] This possibility might also explain the two time scales of photobleaching that were observed in the epifluorescence ensemble measurements. While the faster rate may represent the photobleaching of the intact protein, the slower rate may denote the bleaching rate for a chromophore that can dissipate its excited-state energy via nonradiative and nondamaging mechanisms.

To develop the coupled-chromophore model, prior work on energy transfer in weakly coupled multichromophoric proteins with comparable interchromophore distances, such as chlorophyll-substituted hemoglobin, serves as a guide.[9,15] The distances and orientations of the individual chromophores in the *Ds*Red complex are now known from X-ray crystallographic data.[18] The chromophores, arbitrarily numbered 1 through 4, are assumed to couple by standard dipole−dipole Förster energy transfer.[5,11] This model, involving degenerate energy transfer from one subunit to another chemically identical subunit, can be tested by comparison with the measured ensemble steady-state anisotropy. While the emission spectrum of each subunit is anticipated to be the same, the fixed angles between the chromophores result in a loss of polarization information as the energy is redistributed among the subunits.

First, the coupling between each pair of chromophores in the tetramer is considered. Using estimated mean distances and angles from the crystallographic data, the pairwise rates of energy transfer k_{ij} were calculated from the standard expression

$$k_{ij} = \frac{Q_D \kappa_{ij}^2}{\tau_f d_{ij}^6}\left(\frac{9000(\ln 10)}{128\pi^5 N n^4}\right)\int_0^\infty F_D(\lambda)\epsilon_A(\lambda)\lambda^4 d\lambda$$

For the overlap integral, measured acceptor absorption (ϵ_A) and donor emission (F_D) spectra were utilized, in which the absorbance values were converted to molar extinction coefficients using a maximum ϵ of 75 000 at 558 nm.[1] The fluorescence lifetime (τ_f, 3.6 ns) and the donor quantum yield (Q_D, 0.69) were taken from the present work. Orientational factors (κ_{ij}^2) and interdipole distances (d_{ij}) were calculated from crystallographic data. In these calculations, we assume that the absorption transition dipole moment of each chromophore lies roughly parallel to both the plane of the benzylidineimidazolinone group and to the line joining the hydroxyl and carbonyl atoms of this group in agreement with single-crystal polarized absorption experiments on the GFP mutant S65T (Rosell and Boxer, to be submitted). Further, we assume that the absorption and emission transition dipole moments for each chromophore are parallel, consistent with the measured polarization ratio for monomeric GFP.[24] The resulting values for these parameters and for the rates (k_{ij}, relative to the fluorescence emission rate k_F) are presented in Table 1. The refractive index (n) of the medium between the fluorophores was assumed to be 1.4.[11] Finally, the total anisotropy is calculated from:

$$r = \frac{1}{4}\sum_{i=1}^{4}\sum_{j=1}^{4}\int_{t=0}^{\infty}\frac{r_{ij}}{\tau_f}P_{j|i}(t)dt \qquad \text{where } r_{ii} = r_0 \text{ and}$$

$$r_{i\neq j} = \frac{1}{5}(3(\vec{e}_i \cdot \vec{e}_j)^2 - 1)$$

the vector $\boldsymbol{e_i}$ defines the transition dipole direction of chromophore i, and $P_{j|i}(t)$ is the calculated probability that the photon is localized to chromophore j as a function of time, given initial excitation at chromophore i, and subsequent energy transfer at the rates given in Table 1. r_{ij} is the anisotropy characteristic of absorption at dipole i and eventual emission at dipole j. The time-dependent probabilities $P_{j|i}(t)$ were calculated by solving a straightforward set of four coupled differential equations describing inter-chromophore coupling (k_{ij}) and emission processes.

Because the rates of energy transfer are considerably faster than the rate of fluorescence emission (see Table 1), an absorbed photon has a nearly equal probability of eventual emission from any of the four subunits. As a result, the measured ensemble anisotropy of *Ds*Red is considerably lower than the largely homologous but monomeric GFP due to the loss of polarization information during this redistribution. The calculated bulk anisotropy from the model above (0.18) is slightly higher than a system where the emission is equally likely from all chromophores (0.17) but somewhat lower than the measured value of 0.23. The differences probably result from the approximations of distance and orientation from the crystallographic model. In any case, this calculation suggests that the reduction in anisotropy appears to result from energy transfer effects.

Although a process involving exciton coupling between the monomers in a complex was considered as a fourth alternative process, the absence of the sharp split of the Cotton effects in the visible region of the CD spectrum of the protein indicates that this mode is insignificant.

In this paper, the photophysical behavior of wild-type *Ds*Red in the ensemble and single-molecule regimes has been described. The system provides much larger numbers of emitted photons than current GFP mutants, approaching the values from some fluorescent dyes.[20] At the single-molecule level, the observed multistep emission traces are likely due to the tetrameric character of the complex, combined with the possibility that the chromophores in the complex are coupled by dipole−dipole energy transfer. The possible advantages of *Ds*Red, namely, long-wavelength emission, reduced photobleaching, environmental insensitivity, and high fluorescence quantum yield argue strongly for further improvement of this chromophore. However, the tetramerization behavior and slow maturation,[7] while not detrimental to all experiments, can pose problems in some situations. Efforts to curtail this oligomerization through mutagenesis along the complex's interfaces could therefore also expand the utility of this promising label.

Acknowledgment. We thank J. Remington for crystallographic coordinates in advance of publication, and R. Y. Tsien for advance copies of publications refs 7 and 1 and the expression system pRSET$_b$-GFP. This material is based upon work supported by the National Science Foundation under Grant No. MCB-9816947 (W.E.M.) and by the National Institutes of Health under Grant GM27738 (S.G.B.) B.L. thanks NATO for Fellowship support, and F.I.R. acknowledges a postdoctoral fellowship from NSERC.

References and Notes

(1) Baird, G. S.; Zacharias, D. A.; Tsien, R. Y. *Proc. Nat. Acad. Sci. U.S.A.* **2000**, *97*, 11984−11989.

(2) Bublitz, G.; King, B. A.; Boxer, S. G. *J. Am. Chem. Soc.* **1998**, *120*, 9370−9371.

(3) Bublitz, G. U.; Boxer, S. G. *Ann Rev. Phys. Chem.* **1997**, *48*, 213−242.

(4) Cantor, C. R.; Schimmel, P. R. *Biophysical Chemistry*; W. H. Freeman: San Fransisco, 1980; Vol. 2.

(5) Clegg, R. M. Fluorescence Resonance Energy Transfer. In *Fluorescence Imaging Spectroscopy and Microscopy*; Wang, X. F., Herman, B., Eds.; Wiley: New York, 1996; Vol. 137; pp 179−252.

(6) Dickson, R. M.; Cubitt, A. B.; Tsien, R. Y.; Moerner, W. E. *Nature* **1997**, *388*, 355.

(7) Gross, L. A.; Baird, G. S.; Hoffman, R. C.; Baldridge, K. K.; Tsien, R. Y. *Proc. Nat. Acad. Sci. U.S.A.* **2000**, *97*, 11990−11995.

(8) Heikal, A. A.; Hess, S. T.; Baird, G. S.; Tsien, R. Y.; Webb, W. W. *Proc. Nat. Acad. Sci. U.S.A.* **2000**, *97*, 11996−12001.

(9) Kuki, A.; Boxer, S. G. *Biochemistry* **1983**, *22*, 2923−2933.

(10) Kumble, R.; Hochstrasser, R. *J. Chem. Phys.* **1998**, *109*, 855−865.

(11) Lakowicz, J. R. *Principles of Fluorescence Spectroscopy*; Kluwer Academic: New York, 1999.

(12) Lu, H. P.; Xun, L.; Xie, X. S. *Science* **1998**, *282*, 1877−1882.

(13) Matz, M. V.; Fradkov, A. F.; Labas, Y. A.; Savitsky, A. P.; Zaraisky, A. G.; Markelov, M. L.; Lukyanov, S. A. *Nat. Biotechnol.* **1999**, *17*, 969−973.

(14) Moerner, W. E.; Orrit, M. *Science* **1999**, *283*, 1670−1676.

(15) Moog, R. S.; Kuki, A.; Fayer, M. D.; Boxer, S. G. *Biochemistry* **1984**, *23*, 1564−1571.

(16) Peterman, E. J. G.; Brasselet, S.; Moerner, W. E. *J. Phys. Chem. A* **1999**, *103*, 10553−10560.

(17) Rees, D. A. *Biochem. J.* **1972**, *126*, 257−273.

(18) Yarbrough, D.; Wachter, R. M.; Kallio, K.; Matz, M. V.; Remington, S. J. *Proc. Nat. Acad. Sci. U.S.A.* **2001**, *98*, 462−467.

(19) Sambrook, J.; Fritsch, E. F.; Maniatis, T. *Molecular Cloning: A Laboratory Manual*; Cold Spring Harbor Laboratory Press: Cold Spring Harbor, New York, 1989.

(20) Soper, S. A.; Nutter, H. L.; Keller, R. A.; David, L. M.; Shera, E. B. *Photochem. Photobiol.* **1993**, *57*, 972−977.

(21) Swaminathan, R.; Hoang, C. P.; Verkman, A. S. *Biophys. J.* **1997**, *72*, 1900−1907.

(22) Tsien, R. Y. *Annu. Rev. Biochem.* **1998**, *67*, 509−544.

(23) VanDen Bout, D. A.; Yip, W. T.; Hu, D.; Fu, D. K.; Swager, T. M.; Barbara, P. F. *Science* **1997**, *277*, 1074−1077.

(24) Volkmer, A.; Subramanian, V.; Birch, D.; Jovin, T. *Biophys. J.* **2000**, *78*, 1589−1598.

(25) Weiss, S. *Science* **1999**, *283*, 1676−1683.

(26) Xie, X. S.; Trautman, J. K. *Annu. Rev. Phys. Chem.* **1998**, *49*, 441−480.

(27) Zacharias, D. A.; Baird, G. S.; Tsien, R. Y. *Curr. Opin. Neurobiol.* **2000**, *10*, 416−421.